Magnetic flux ropes and space weather

A. Nindos

Physics Department, University of Ioannina, Greece

Work done with S. Patsourakos, A. Vourlidas, X. Cheng, J. Zhang, S. Koya

Overview

- Pre-eruptive magnetic configurations
- Magnetic flux rope proxies
- Hot channels/hot blobs as evidence of hot magnetic flux ropes
- Detection of hot flux ropes in a large sample of M- and X-class flares
- When do erupting hot flux ropes form?
- Magnetic clouds
- The space weather connection: near-Sun magnetic field of erupting flux ropes

Pre-eruptive Magnetic Configurations

- BUT all models predict that the CME will contain a flux rope after eruption
- While the flux rope is an integral part of the pre-eruptive configuration in the first group of models, it forms during the eruption in the second group of models.

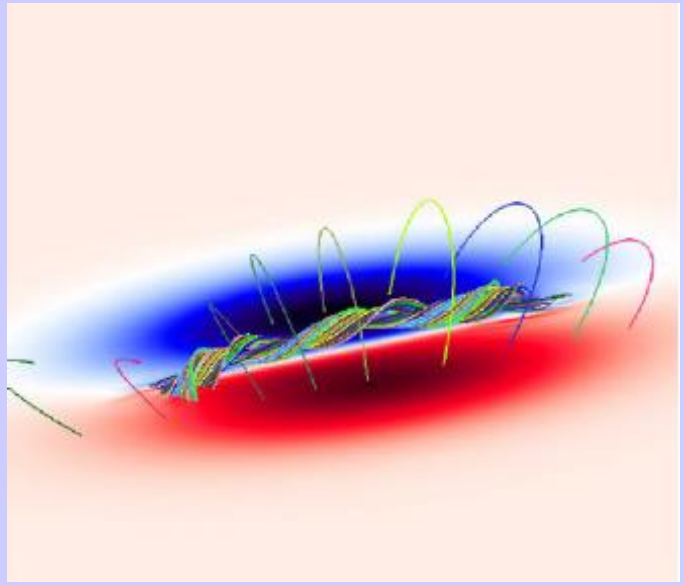

Magnetic Flux Rope

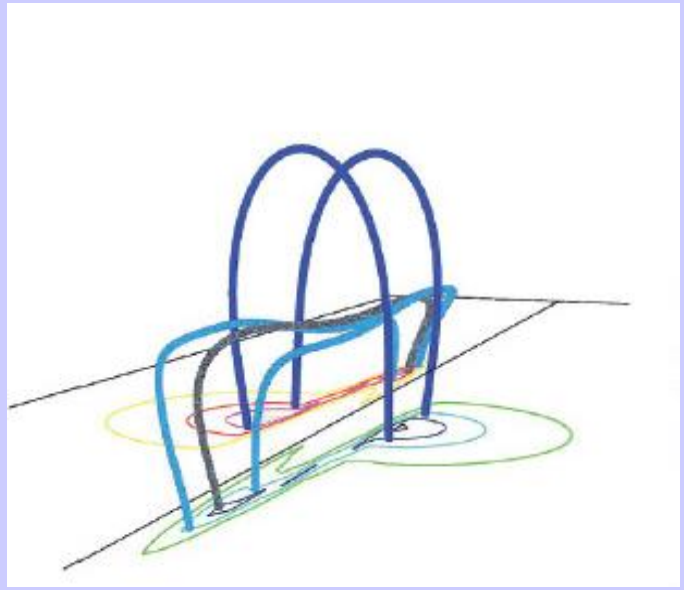

Sheared Arcade

Magnetic flux rope proxies

Braided structure within filament

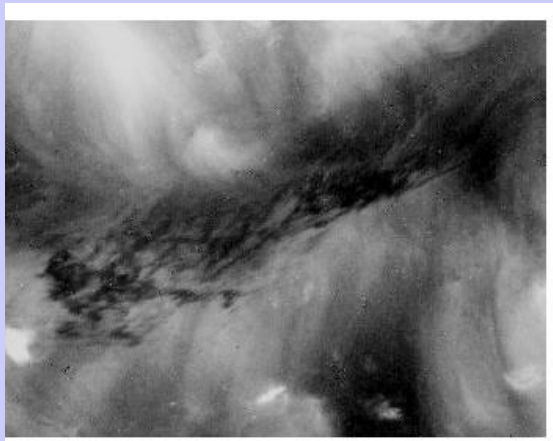

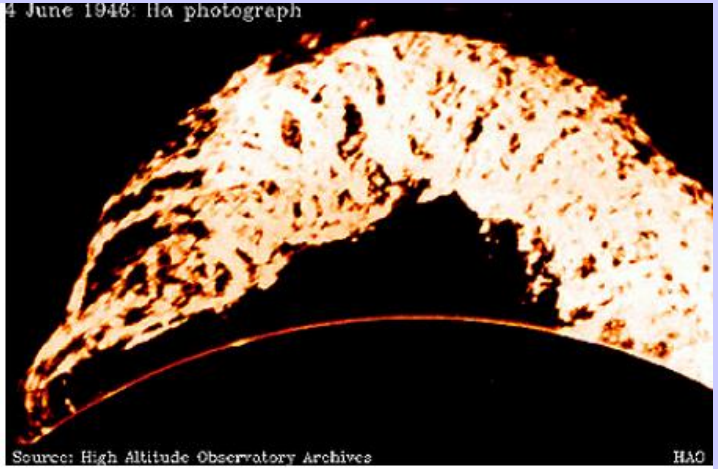

Helical structure in erupting prominence

Formation of a sigmoid from an increasingly sheared arcade (Green et al. 2011)

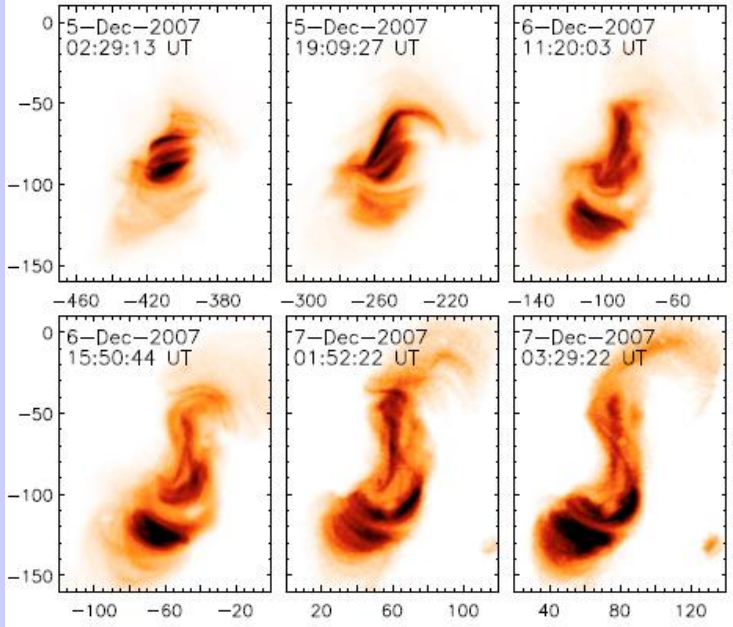

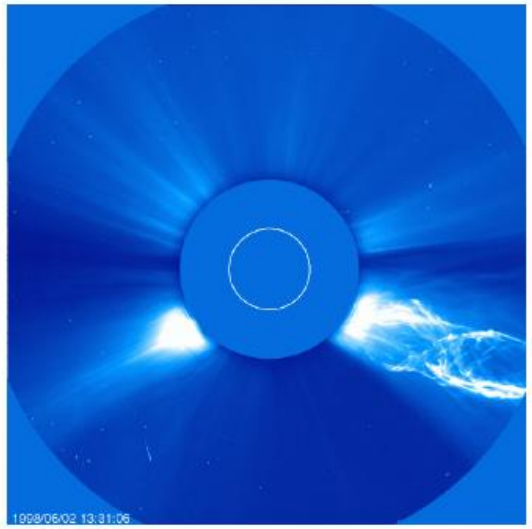

CME with helical structure

Magnetic flux rope proxies

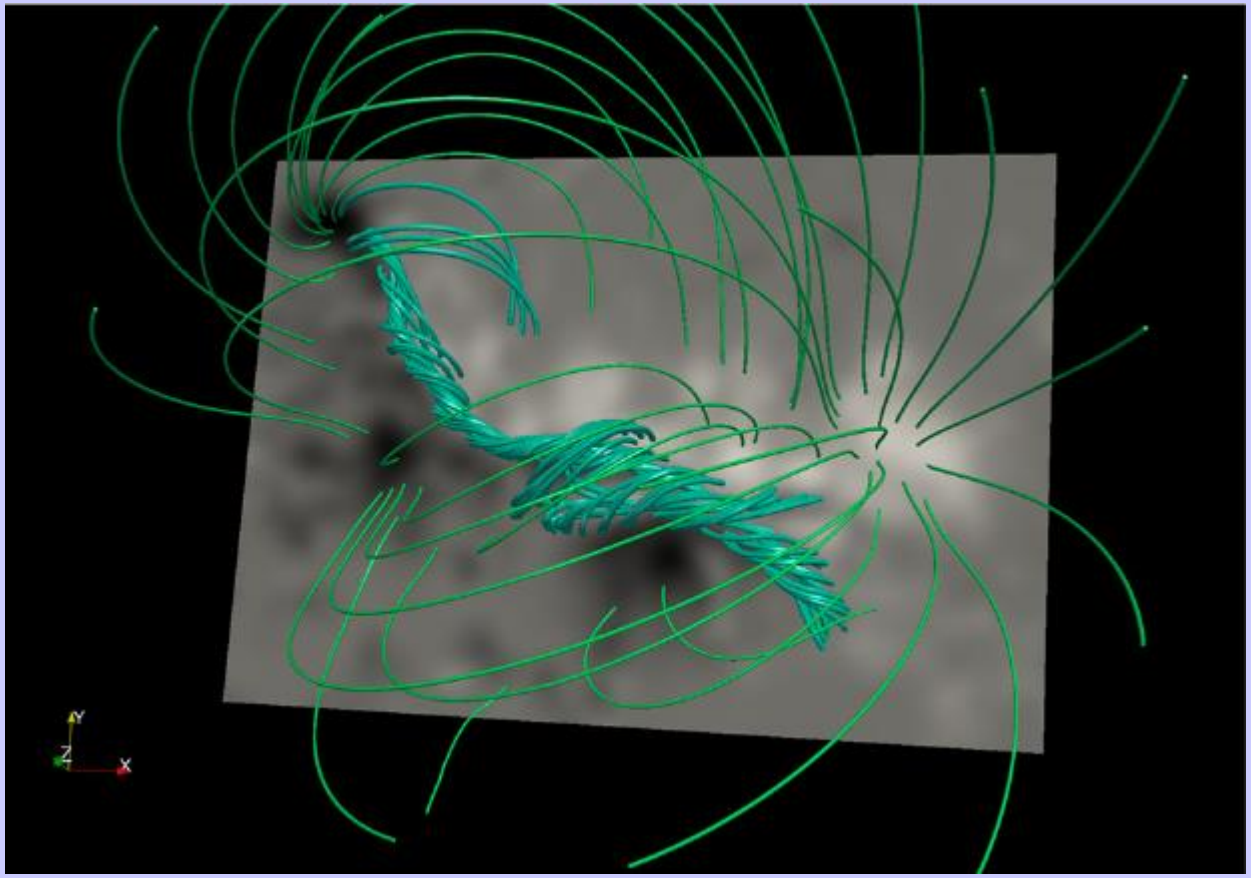

Chintzoglou et al. (2015)

NLFFF extrapolations

Magnetic flux rope proxies

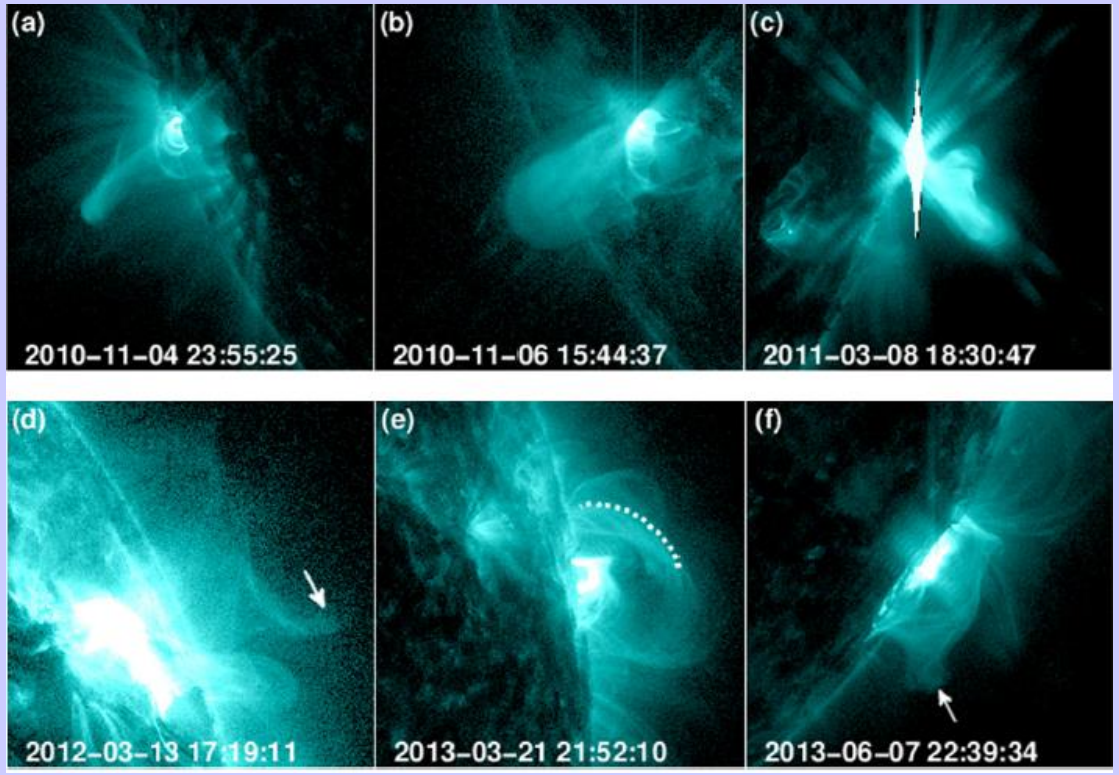

Examples of hot flux ropes (HFRs) from AIA/SDO images at 131 A

How common are hot flux ropes in the low corona?

- Database of 141 M-class and X-class flares that occurred at longitudes > 50^{o}
- Half of the flares were associated with CMEs
- Goal of the survey: assess the frequency of hot flux ropes in large flares irrespective of their formation time relative to the onset of eruption
- The flux ropes were identified in 131 Å images using morphological criteria and their high temperatures were confirmed by their absence in the cooler 171 and 304 Å passbands.

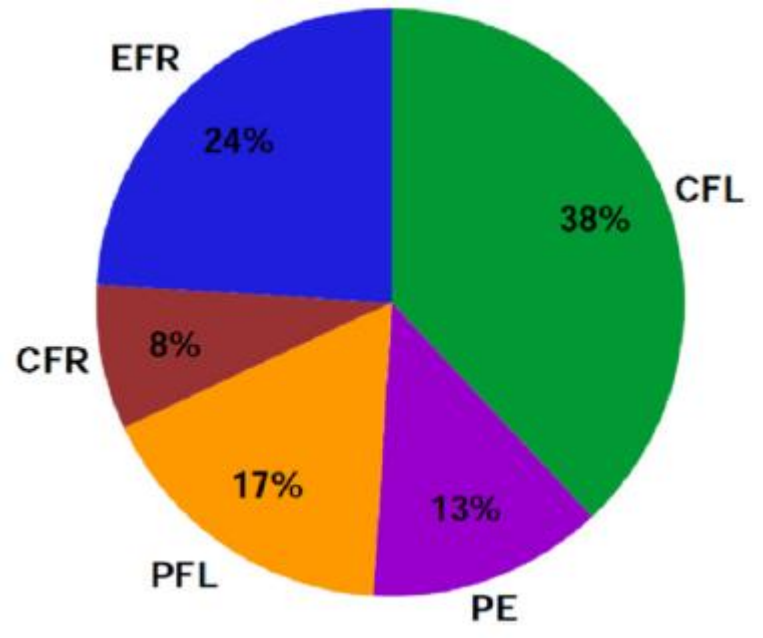

- CFR: Confined flare events with hot flux ropes
- EFR: Eruptions with hot flux ropes
- PE: Prominence eruptions without hot flux ropes
- PFL: Eruptions without hot hot flux ropes or prominences
- CFL: Confined flare events without hot flux ropes

- **Hot flux ropes in 45 of our events (32% of the flares)**
- **11 of them were associated with confined flares while the remaining 34 were associated with eruptive flares.**
- **-> almost half (49%) of the eruptive events involved a hot flux rope configuration.**

When do erupting hot flux ropes form?

- 34 eruptive M/X-class limb flare events that involved an HFR configuration
- Create uninterrupted sequences of 131 Å AIA images that spanned >8 hrs, ending a few minutes after the onset of the eruption
- Morphological criteria for the identification of and for monitoring the evolution of the flux ropes
- Ensure that all candidate FRs were hot by their absence in 171 and 304 Å data
- Further confirm the existence of the FRs by checking out 8-hr-long movies of AIA data at 94, 193, 211, and 335 Å AIA data

- Search for confined flares associated with the appearance of the HFRs that later erupted (Patsourakos+ 2013)

Purpose of the timing study

- A few previous case studies on the formation times of hot flux ropes (HFRs). Their main focus: whether the FR forms before or during the eruption
- Case studies do not address the statistics of the formation times of HFRs in eruptive events
- Present study: Determine the formation times of HFRs with respect to the eruption in an extensive dataset of large eruptive events using observations that cover several hours before the onset of the eruptions.

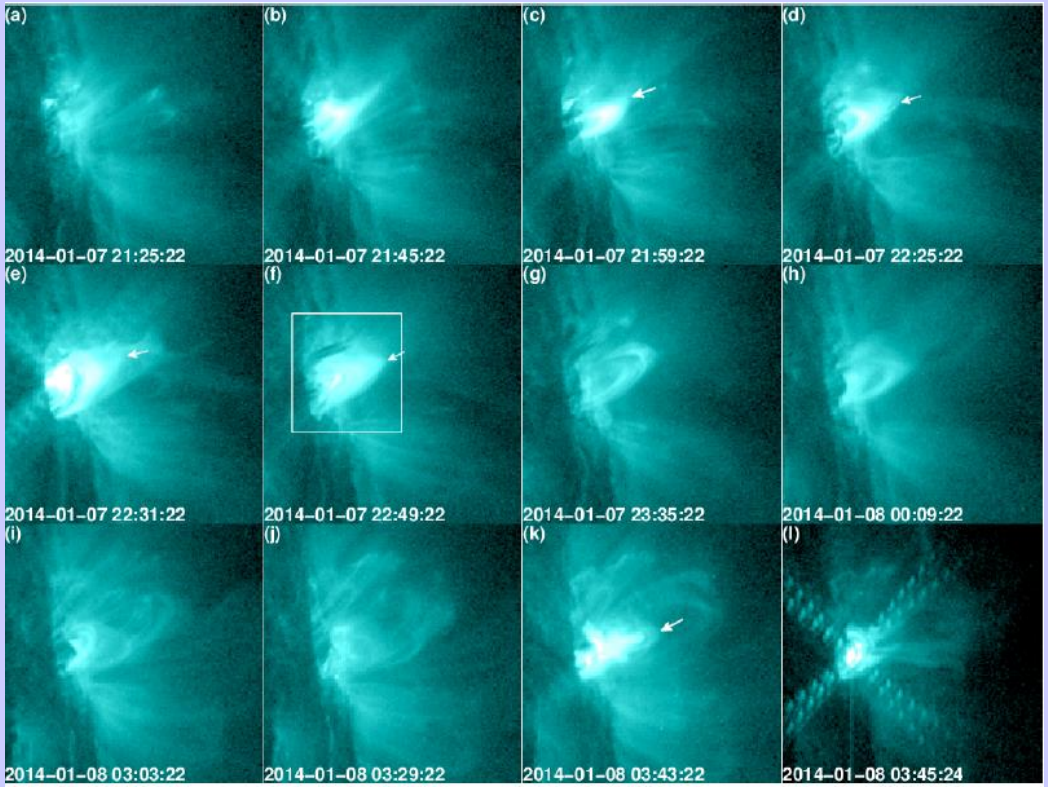

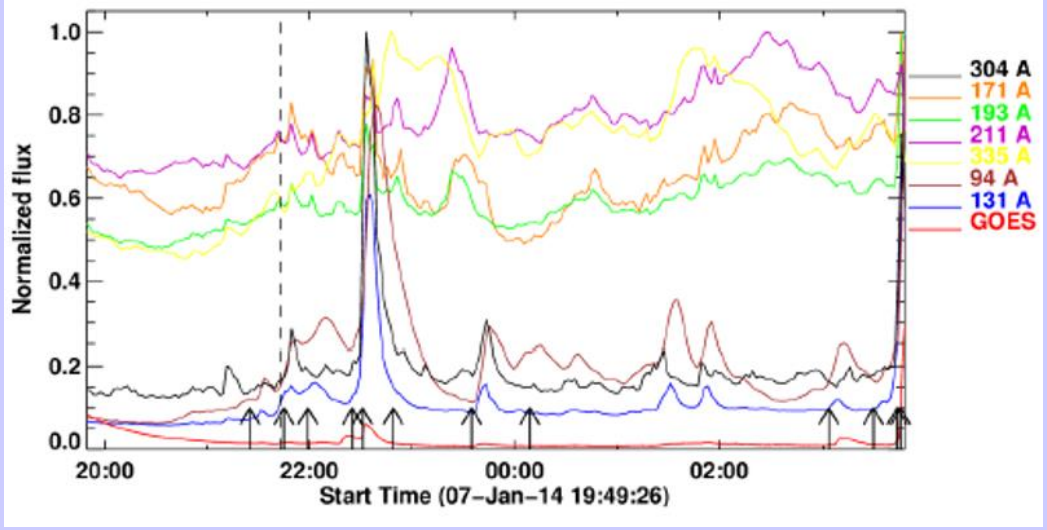

Example: Pre-existing HFR whose formation was associated with a confined flare (PREC)

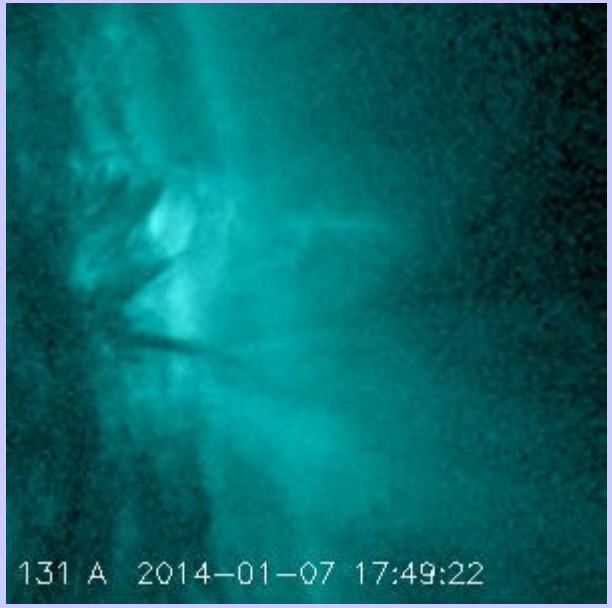

Conclusions of the flux rope timing study

Table Statistics of the patterns of HFR formation.

Classification[(a)]	Range of Δt[(b)] (min)	Number of events
FLY	[−5, −2]	3
FLYP	[−3, 0]	3
PRE	[3, 39]	4
PREC	[51, 536]	20
UNC	–	4

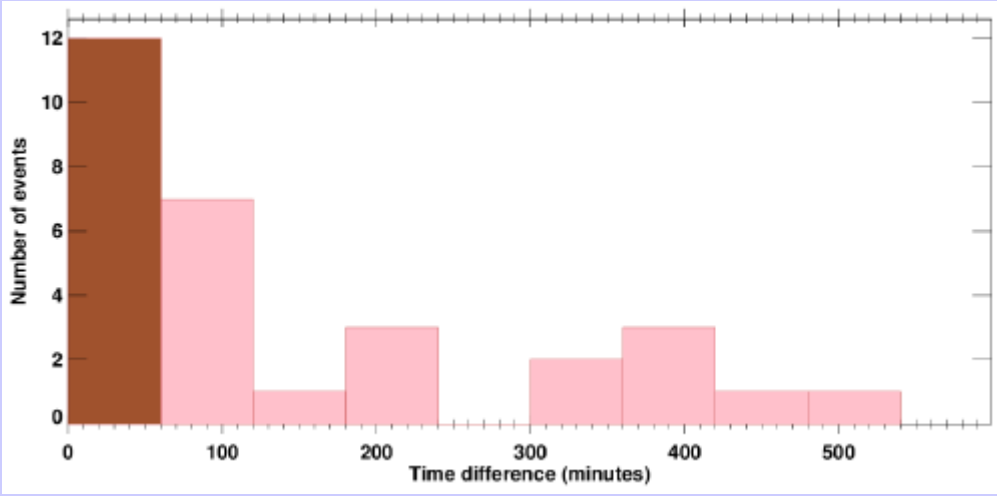

Histogram of the number of events versus the time difference btw the onset of the eruptive flare and the appearance of the HFR

- FLY: HFR formed during the event without pre-existing prominence material
- FLYP: HFR formed during the event with pre-existing prominence material
- PRE: Pre-existing HFR whose formation was not associated with a confined flare
- PREC: Pre-existing HFR whose formation was associated with a confined flare
- UNC: Uncertain events

Our results provide, on average, indirect support for CME models that involve pre-existing flux ropes

- Two-thirds (20/30) of the HFRs were formed well before the onset of the eruption (from 51 min to >8 hrs) and their formation was associated with the occurrence of a confined flare
- 4 events with pre-existing HFRs whose formations occurred a matter of minutes (3-39) priorto the eruptions without any association with confined flare activity
- 6 HFRs were formed once the eruptions were underway (but in 3 of them prominence material could be seen in 131 Å images)

Magnetic clouds: flux ropes in the IP space

Magnetic clouds (MCs) can be distinguished by:

- Relatively strong magnetic field
- Large and smooth B-field rotation
- Lower proton temperature than average

<u>In the figure:</u>

- The MC is observed in the interval btw the two vertical green lines
- The MC is driving a shock (S) denoted by the vertical blue line

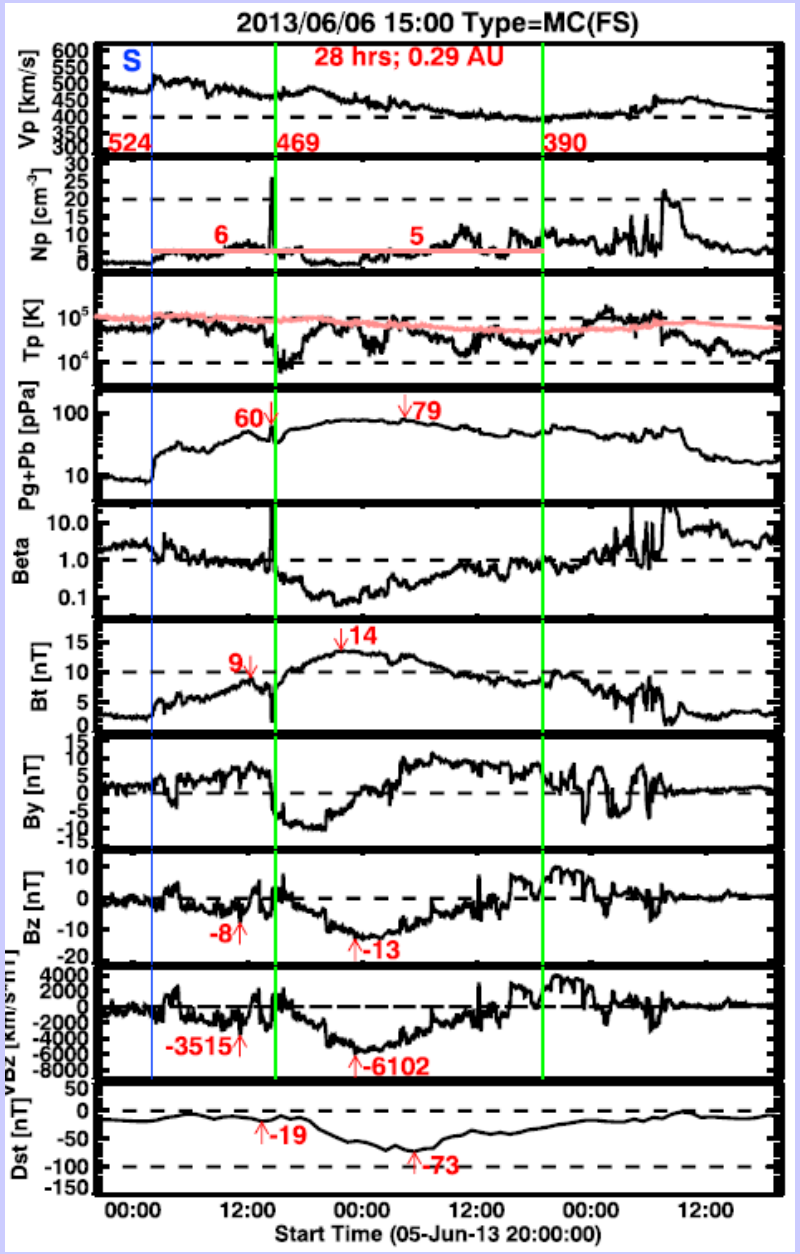

Plasma flow speed

Proton density

Proton temperature

Total pressure ($P_g + P_b$)

Plasma beta

Total magn. field strength

B_y

B_z

VB_z

Dst index

Gopalswamy et al. (2015)

Assessment of axial magnetic field of the CME observed on 10 March 2022 from AR Helicity budget

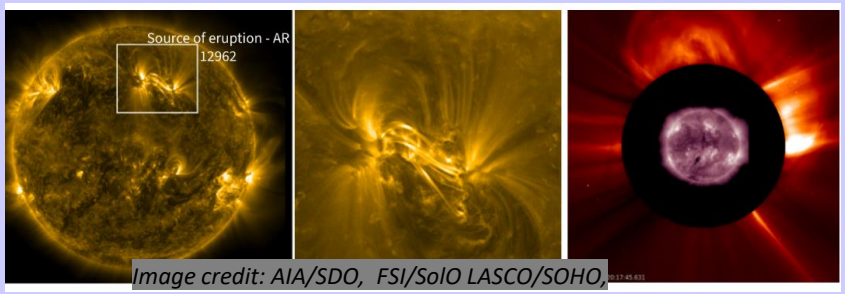

Image credit: AIA/SDO, FSI/SolO LASCO/SOHO

Conservation of Magnetic helicity: CMEs appear a necessity for the solar corona to act as a valve to relieve excess helicity from the Sun.

- SolO remote and in-situ observations of the ICME at 7.8° East of the Sun-Earth line at a heliocentric distance of 0.43 AU.
- From AR 12962, C2.8 flare in NW quadrant

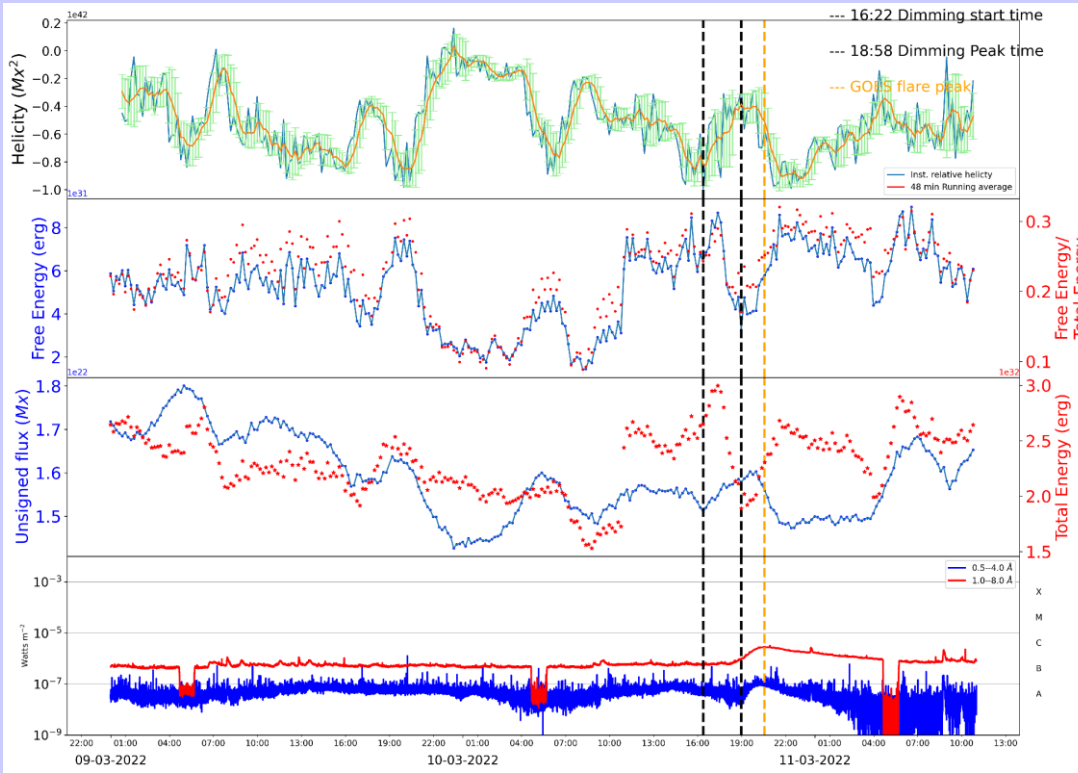

Calculation of instantaneous relative magnetic helicity using connectivity based method from photospheric vector magnetograms (Georgoulis et al, 2012) :

Helicity variation

- A decreasing phase of relative magnetic helicity starting from 10 March 16:22 UT to 18:58 UT.
- The net helicity value continuously decreased from -9.946×10^{41} $\pm 1.48 \times 10^{41}$ Mx^2 to $-2.793 \pm 0.70 \times 10^{41}$ Mx^2
- The difference in helicity accumulated in the AR nearly start time of dimming to peak dimming time is $-7.153 \pm 1.63 \times 10^{41}$ Mx^2

Free energy variation

- The difference free energy between 16:22 UT (start time of decrease) and 18:58 UT is 4.56×10^{31} erg

The difference in source region helicity is assumed to be bodily transported to the associated CME.

From source AR helicity to CME Bz

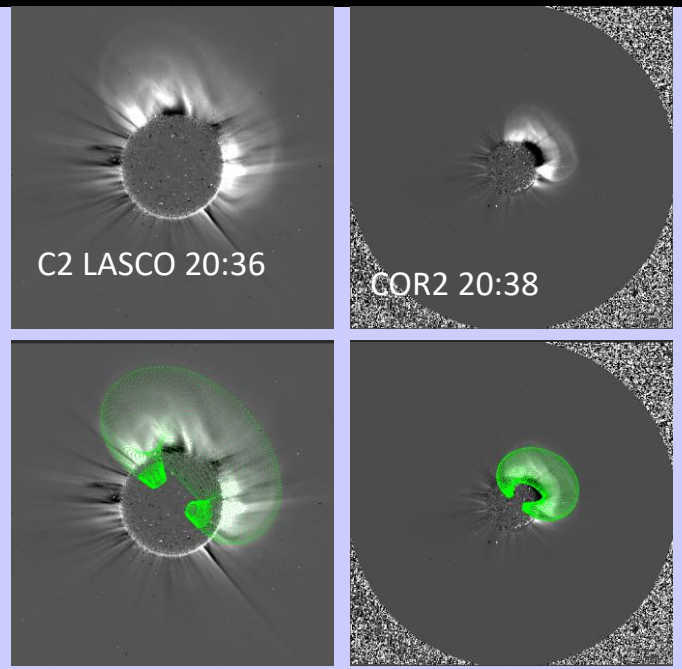

GCS model in Thernisien et al. (2008) in COR2, C2 observation.

Height = 7.64 Rs
Aspect ratio = 0.31
Half angle = 55.62 deg

- Axial magnetic field and magnetic helictiy of of a cylindrical flux rope is related as:*DeVore 2000, Demoulin et al 2022, Dasso et al 2003, Berger et al 2003*

$$H_m = 0.7\, B_0^2\, R_0^3\, L \quad \text{----------(1)}$$

- We used monte- carlo simulation for estimation of uncertainty involved in CME Bz
- Estimated CME Bz at coronal height of 7.64 R_s= 2067 ± 405 nT

Extrapolation of CME Bz by power law of heliocentric distance and In-situ observations

In-situ observation from MAG/SolO at 0.43 AU and WIND at 1 AU

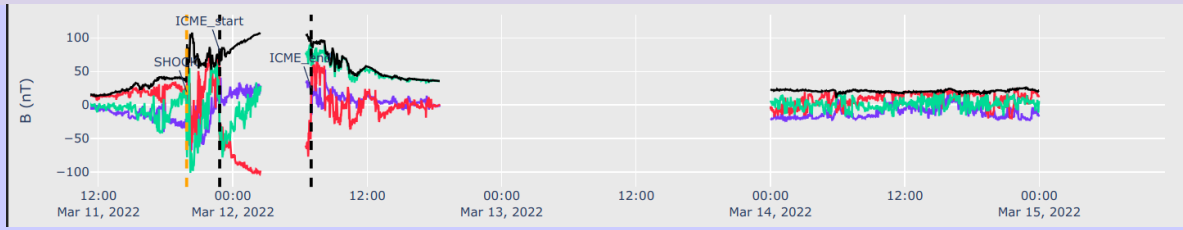

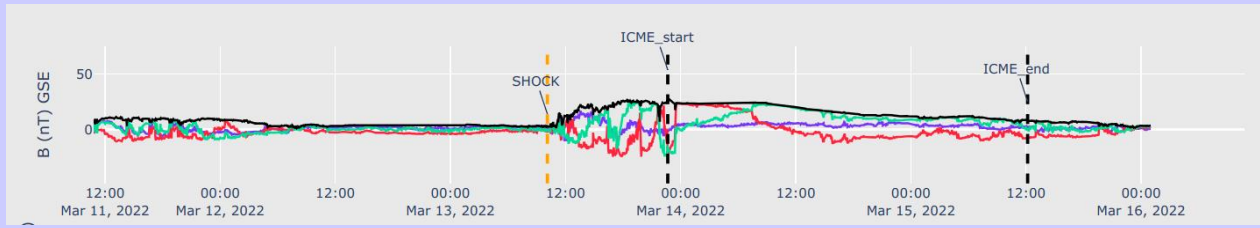

From Patsourakos 2016:

$$B_0(r) = B_* (r/r_*)^{aB} \quad \text{----------(2)}$$

- ICME peak B at 0.43 AU from MAG/SolO= 97.12 nT
- ICME peak B at 1 AU from WIND=24.41 nT
- Estimated power law index from 7.64 R. to 0.43 AU from eqn (2)= -1.22
- Estimated Power law index from 0.43 AU to 1 AU from in-situ observations= -1.63

Koya et al. (2023, in preparation)

The space weather connection: Conclusions of the CME axial magnetic field study

- Use magnetic helicity to constrain the CME axial magnetic field in the low corona
- Use a power-law to extrapolate the low corona magnetic field into a heliospheric distance for which in situ Bz measurements are available
- The resulting distribution of the near-Sun (at ~10 Rs) CME magnetic fields varies in the range [400, 2000] nT
- For power-law indices varying in the range [−1.9, −1.4], we obtain a considerable ballpark agreement with MC magnetic-field measurements at 1 AU